sciendo

Polish Journal of Chemical Technology, 26, 4, 56—63, 10.2478/pjct-2024-0040

Ball milling preparation of spent graphite supported zero-valent iron-copper to degrade tetracycline in water

Xingping Hang[1, 2, 3], Xiaotian Wu[4], Wei Song[3], Shuai Chen[1, 2*]

[1]Anhui International Joint Research Center for Nano Carbon-based Materials and Environmental Health, Anhui University of Science & Technology, Huainan 232001, China
[2]School of Resources and Environmental Engineering, Shanghai Polytechnic University, Shanghai 201209, China
[3]Shanghai Zhongran Marine Fuel Co., LTD, Shanghai 200080, China
[4]Odin Fire Equipment Co., LTD, Shanghai 201600, China
[*]*Corresponding author: e-mail:* chenshuai@sspu.edu.cn

In this study, graphite and copper from spent LIBs were used to prepare graphite supported zero-valent iron-copper (ZVI-Cu/G) by ball milling, to improve the reactivity of ZVI. The structure, composition, morphology, and properties of ZVI-Cu/G were fully analyzed. The removal performances of tetracycline by ZVI-Cu/G were tested under different reaction conditions. Graphite and copper improve the dispersion, specific surface area and reactivity of the material. Operational factors, material dosage of 1 g/L, initial pH of 3, temperature of 25 °C, and H_2O_2 concentration of 2 mM, contribute to the best tetracycline removal rate, being 100% in 30 min for 30 mg/L tetracycline solution. The reaction data fits a pseudo first-order model. Tetracycline removal rate was as high as 90% even in the 3rd round of reuse. This study reports a novel ZVI material with high tetracycline removal rate.

Keywords: sustainable development, Schiff bases, green chemistry, green synthesis.

INTRODUCTION

As an energy storage device, lithium ion battery (LIB) has been widely used in electronic products and electric vehicles. China has become the world's largest manufacturer of LIBs, and 940 GWh LIBs was produced in 2023. Due to the rapid upgrading of electronic products and electric vehicles and the limited service life, generally 1–3 years, of LIBs, the explosive growth of LIBs has generated a large amount of spent LIBs. The metals, like nickel, cobalt, lithium, etc. in spent LIBs will cause serious pollution to soil and water, threatening environmental safety and human health[1]. By contrast, these metals are resources, and their recycling is important to solve the shortage of metal minerals.

The composition of LIBs mainly includes aluminum shell, circuit board, cathode, anode, plastic film and other components. Because the components of spent LIBs are complex, they can be disassembled and sorted to improve the resource recovery rate[2]. Due to the high value of metals in the cathodes of spent LIBs, more and more research focused on the extraction of metals in cathodes have been conducted, the methods include pyrometallurgy, hydrometallurgy and biological metallurgy[3]. There is a large amount of graphite and copper foil in the anodes of spent LIBs, accounting for 25%∼28% of the total cost of LIBs. At present, however, there are few studies focus on the recovery of graphite and copper in the anodes. Zhao et al.[4] synthesized MnO_2 modified graphite adsorbent from spent graphite to remove heavy metals like Pb, Cd and Ag from water. Nguyen and Oh[5] used graphite of spent LIBs in the persulfate/zero-valent iron (ZVI) system, and found that graphite could enhance the oxidation of persulfate and the reduction of ZVI.

In recent years, antibiotics have been increasingly used for veterinary and medical purposes. Among them, tetracycline has a widely application in the treatment of a variety of infectious diseases because of its broad antibacterial action. Most of the antibiotics taken cannot be fully absorbed by the body and will be excreted in urine and feces in forms of maternal or metabolite, which will pollute the environment and induce the generation of resistance genes, ultimately posing a potential threat to human health.

Adsorption by, for example, carbon nanotubes, activated carbon, clays, zeolites and metal oxides, et al. have been used to remove tetracycline[6–10]. Selvaraj et al.[11] used activated carbon derived from *Cynometra ramiflora* fruit biomass for tetracycline adsorption. Hamdi et al.[12] used clays to adsorb tetracycline and found that the adsorption potential of clay for tetracycline was close to 100%. Sun et al.[10] used Fe-Mn-Ce metal oxides prepared by using a co-precipitation method for the removal of tetracycline. In addition, ZVI based materials are mainly used in advanced oxidation technology to remove tetracycline by multi-phase Fenton oxidation[13]. However, ZVI is easy to agglomerate due to its inherent magnetism, which reduces its reactivity to remove pollutants. To solve this problem, it is commonly used to load ZVI on carriers or add bimetals to ZVI. Fernández-Velayos et al.[14] used an alternative method based on 3D printing technology to prepare ZVI polylactic acid to activate persulfate for tetracycline removal in cyclic mode under thermal bath. Zhang et al.[15] found that the Fe-Cu bimetallic catalyst is far superior to the single metal catalyst in catalytic performance. However, the electrical conductivity of supported ZVI materials and bimetallic materials constructed by existing loading methods decreases after passivation. Thus, it is still necessary to further improve their reactivity.

It is of great significance to construct graphite-loaded zero-valent iron-copper bimetal (ZVI-Cu/G) with ZVI and anodes from spent LIBs by ball milling method, which can not only obtain the efficient recovery of spent LIBs, but also produce high reactive and cheap ZVI material. In this paper, graphite and copper foil were efficiently recovered from the anode of spent LIBs, and graphite-loaded ZVI and ZVI-Cu materials were prepared by ball milling method. The tetracycline removal ability was

investigated under different conditions, and the removal mechanism of tetracycline was speculated.

MATERIALS AND METHODS

Materials

ZVI (≥99.0%), cellulose (≥99.0%), hydrochloric acid (36%) and hydrogen peroxide (30%) were obtained from Sinopharm Chemical Reagent Co. Ltd. Tetracycline (≥99.0%) was obtained from the Shanghai Lingfeng Chemical Co. Ltd. The anode of spent LIB (BL-5J) was roasted separately at 500 °C in nitrogen for 1 h, and the graphite and copper foil were separated by manually shaking.

Methods

Synthesis of ZVI/G and ZVI-Cu/G

The graphite from the anode of spent LIBs and ZVI were fully mixed according to graphite and ZVI mass ratios of 1:1, 1:2 and 1:3, with the rotational speed of 400 rpm and ball milling time of 5 h, and these three materials were named as ZVI/G-1, ZVI/G-2 and ZVI-/G-3, respectively. The ZVI-Cu/G material was prepared by adding 0.96% copper foil in the raw material when preparing the ZVI/G-2.

Characterization of materials

The crystal structure of the graphite, ZVI/G and ZVI-Cu/G materials were analyzed with a Bruker D8 Advance X-ray diffractometer (XRD) by using the CuKα radiation, operated at 40 kV, with the step size of 0.02° and the scanning range of 10 ~ 80°. Surface morphology of the ZVI/G and ZVI-Cu/G materials were tested by using the Hitachi S-4800 scanning electron microscope (SEM) at an accelerating voltage of 15 kV. The elemental distributions of the ZVI-Cu/G were determined by using the EDAX TEAM Apollo energy spectrometer (EDS). Moreover, the structure of ZVI-Cu/G was tested by using the JEOL JEM-1400 transmission electron microscopy (TEM), operated at an accelerating voltage of 120 kV. The porous structure of the ZVI/G and ZVI-Cu/G materials was tested by N_2 adsorption/desorption at –196 °C by using a Micromeritics TriStar 123 static volumetric system, after the samples vacuum degassed at 150 °C for 6 h. The specific surface areas were calculated by using the Bruner-Emmett-Taylor (BET) equation. The functional groups in the materials were analyzed by using the Thermal Fisher Scientific Nicolet 6700 Fourier transform infrared spectrometer (FT-IR) in the frequency range of 400–4000 cm^{-1}, after the treatment of samples with KBr pressing method.

Degradation of tetracycline with ZVI/G and ZVI-Cu/G materials

The 100 mL of tetracycline solution with a concentration of 30 mg/L was added to a 250 mL conical flask, H_2O_2 and the ZVI/G or ZVI-Cu/G were then added and the mixture was shaken well. The 1 mL of the water sample was taken at various time intervals and immediately placed in 1 mL of methanol to stop the chemical reaction, and the concentrations of tetracycline and by-products were tested with a Shimadzu liquid chromatography-mass spectrometry (LC-MS) instrument according to the methods of USEPA3510C-1996 and USEPA8270E-2018. All experiments were performed three times and averaged. The factors of pH value (3, 5, 7 and 9, adjusted by using 0.1 M HCl or NaOH), hydrogen peroxide concentration (0.5 mM, 1.0 mM, 2.0 mM, 4.0 mM and 7.0 mM), material dosage (0.5 g/L, 0.75 g/L, 1.0 g/L and 1.25g/L) and temperature (15 °C, 25 °C, 35 °C and 45 °C) were investigated, respectively. Metal contents were quantified by using a Thermal Fisher Scientific ICAP700 inductively coupled plasma mass spectrometry (ICP-AES).

The tetracycline degradation data was fitted to the pseudo-first-order as following Eq. 1:

$$-\ln\left(\frac{C}{C_0}\right) = k_1 t \quad (1)$$

where C_0 and C_t are the tetracycline initial concentration and the concentration at time t, respectively, and k_1 is the pseudo first-order rate constant.

RESULTS AND DISCUSSIONS

Characterization of materials

Figure 1 shows the XRD results of graphite, ZVI/G and ZVI-Cu/G materials. At 26.6° (PDF#75-2078) and 44.6° (PDF#87-0721), ZVI/G-1, ZVI/G-2, ZVI/G-3 and ZVI-Cu/G all show significant graphite and ZVI peaks. It can be seen that the peak intensity of graphite in ZVI/G-1, ZVI/G-2 and ZVI/G-3 is significantly weakened, while the characteristic peak of zero-valent iron is gradually strengthened. This is due to the increase of ZVI content in these materials. A peak of 2 Theta = 43.3° (PDF#85-1326) appears in the ZVI-Cu/G material, which can correspond to the (111) crystallographic plane of cubic copper, indicating the successful preparation of ZVI-Cu/G material containing zero-valent copper particles[16].

As shown in Figure 2, the functional groups on the surface of the graphite, ZVI/G-2 and ZVI-Cu/G were analyzed in detail. The bands at 3429 cm^{-1} and 1592 cm^{-1} in both ZVI/G materials and NZVI-Cu/G materials showed broad peaks, which may be related to the -OH stretching vibration[17]. The absorption bands appeared

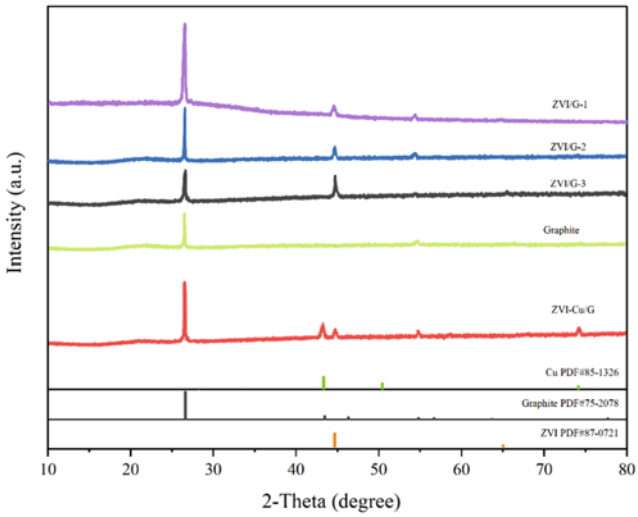

Figure 1. The XRD patterns of graphite, ZVI/G and ZVI-Cu/G materials

near 1640 cm^{-1}, 1385 cm^{-1}, and 1100 cm^{-1} were generated by the C=O stretching vibration. These surface functional groups play important roles in the degradation of organic pollutants by assisting in accepting or donor of electrons.

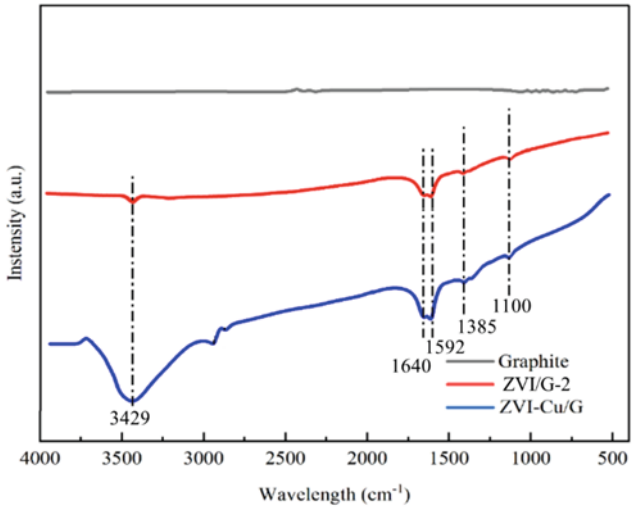

Figure 2. FT-IR patterns of graphite, ZVI/G-2 and ZVI-Cu/G

Table 1. Textual data of ZVI/G and ZVI-Cu/G materials

Sample	S_{BET} (m^2/g)	Average pore diameter (nm)	Pore volume (cm^3/g)
ZVI/G-1	18.6	47.1	0.028
ZVI/G-2	28.3	52.9	0.031
ZVI/G-3	20.6	44.6	0.036
ZVI-Cu/G	40.7	77.4	0.089

Table 1 shows the N_2 adsorption/desorption data of ZVI/G and ZVI-Cu/G materials. The specific surface area of ZVI/G-2 reached 28.3 m^2/g, which was higher than that of ZVI/G-1, being 18.6 m^2/g, and 20.6 m^2/g for ZVI/G-3, indicating that the specific surface area of ZVI/G material will increase with the increase of ZVI content, but the agglomeration effect of ZVI will occur and lead to a decrease in the specific surface area. Because of the addition of Cu, it is found that the specific surface area of ZVI-Cu/G material reaches 40.7 m^2/g, which is the largest among the four materials, indicating that the addition of Cu increases the specific surface area of the material. This may be due to that graphite would be repeatedly struck under the impact force of copper particles, thus forming microstructural defects and increasing surface area[18]. Moreover, the increased surface area may lead to the improvement of the pollutant degradation ability of the material.

As shown in Figure 3a–d, the graphite was more fragmented after ball milling. From (e)–(h), it can be found that the surface of graphite is loaded with ZVI, and the surface of ZVI is densely distributed with copper, which proves that ZVI-Cu/G has been successfully prepared by ball milling. The metal particles exhibited good dispersion in the ZVI-Cu/G material, which expanded the contact surface with pollutants, thus providing more active sites for the reaction and enhancing the reactivity. The TEM results of ZVI-Cu/G are shown in Figure 4. The oval dark particles in the graphite layer are metal and bimetallic particles, while the lighter layers are graphite. The TEM results are consistent with the SEM-EDS results, and these results confirm the successful preparation of graphite supported dispersed ZVI-Cu particles.

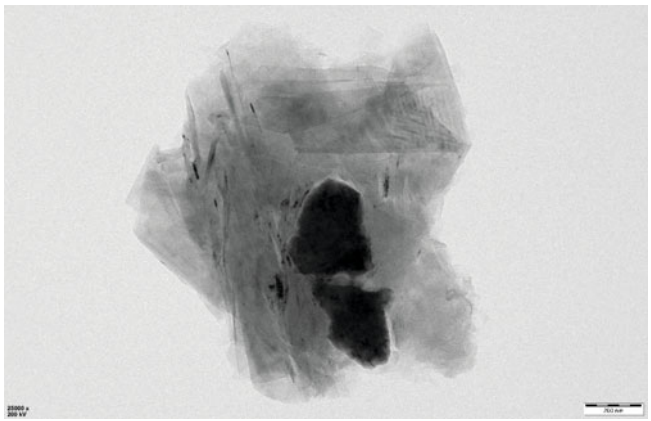

Figure 4. TEM image of ZVI-Cu/G

Tetracycline removal performances by various materials

The performances of different materials for tetracycline removal are shown in Figure 5. Experimental conditions were: Tetracycline concentration of 30 mg/L, hydrogen peroxide concentration of 2.0 mM, pH value of 3, temperature of 25 °C and material dosage of 1.00 g/L. The performance of ZVI-Cu/G was better than that of ZVI/G materials. The tetracycline removal rate reached 91% after 10 min of reaction, and reached 100% after 30 min. Due to the addition of copper, the electron transfer frequency of ZVI in the material is strengthened, so the reaction process is accelerated. Further, it

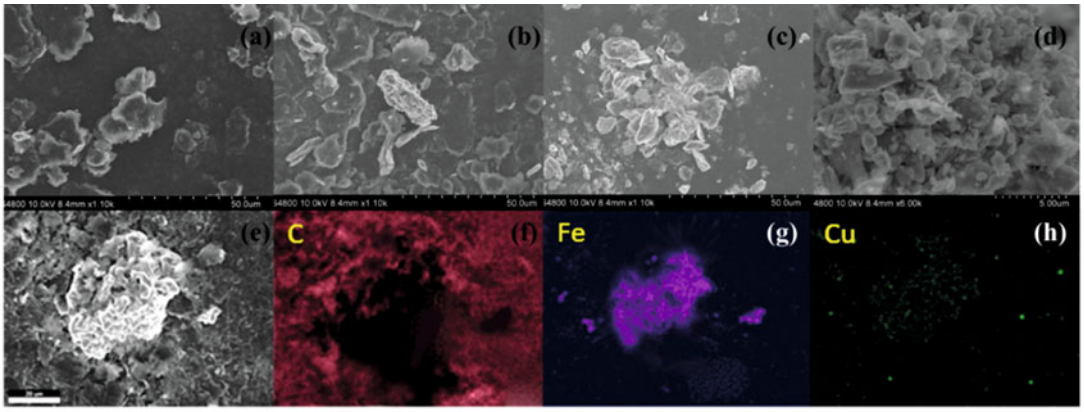

Figure 3. SEM images of (a) ZVI/G-1, (b) ZVI/G-2, (c) ZVI/G-3, (d) ZVI-Cu/G and SEM-EDS images of ZVI-Cu/G (e–h)

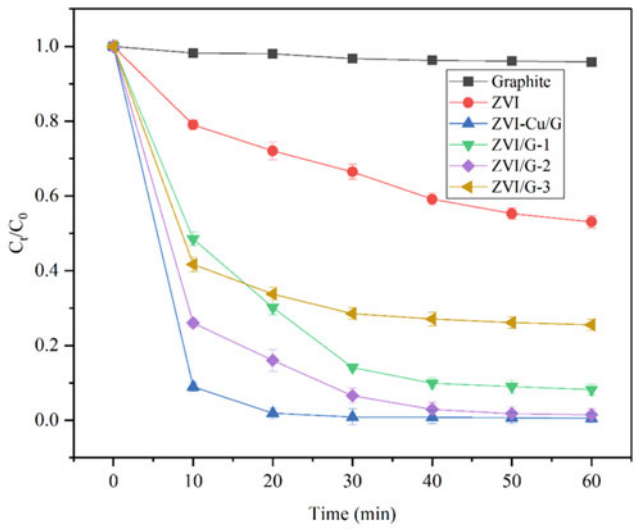

Figure 5. Tetracycline removal performances by various materials

is confirmed that the transition rate of the Fe valence state will increase with the increase of the conductivity in Fe/Cu system[19]. In addition, due to the addition of Cu, the surface of the material was corroded and would work in the Fenton reaction under acidic conditions according to equations 9 and 10[20]. When using ZVI/G-1, the reaction rate was faster in the first 30 min, and the final removal rate reached 92.6%, which may be due to the relatively low ZVI content in ZVI/G-1. When the ZVI content increased, that the material is ZVI/G-3, the tetracycline removal rate only reached 73.8%, and the reaction rate is greatly reduced compared with ZVI/G-2 (98.2%). In acidic solutions, ZVI can generate Fe^{2+} which improves the Fenton process and generate hydroxyl radicals (•OH) by reacting with hydrogen peroxide, thus improving the tetracycline removal performance[21]. The removal performance of organic matter is found to be related to the concentration of Fe^{2+} in solution, the higher the concentration of Fe^{2+}, the faster the reaction rate[22]. However, when the Fe^{2+}concentration reaches a certain degree, its influence on the pollutant removal rate will become smaller and smaller. When the amount of ZVI increases, the particles may agglomerate, resulting in a reduction of the contact area with tetracycline, thus weakening the degradation. Further, with the increase of ZVI amount, the resulting Fe^{2+} may compete with tetracycline for the •OH, reducing the amount of •OH involved in degradation and further affecting the removal rate.

Effects of pH on tetracycline removal by ZVI-Cu/G

To study the effects of initial pH on tetracycline removal by ZVI-Cu/G, the experimental conditions were set that the tetracycline concentration was 30 mg/L, the dosage of ZVI-Cu/G was 1.00 g/L, the temperature was 25 °C, and the concentration of hydrogen peroxide was 2.0 mM. The control variables pH were 3, 5, 7, and 9, respectively, and the results are shown in Figure 6a. The best tetracycline removal rate was achieved when the pH value of the solution was 3, and the removal rate of tetracycline reached 100% within 30 min. It may be because the formation of oxide film on the surface of ZVI is weak under acidic conditions, which reduces the

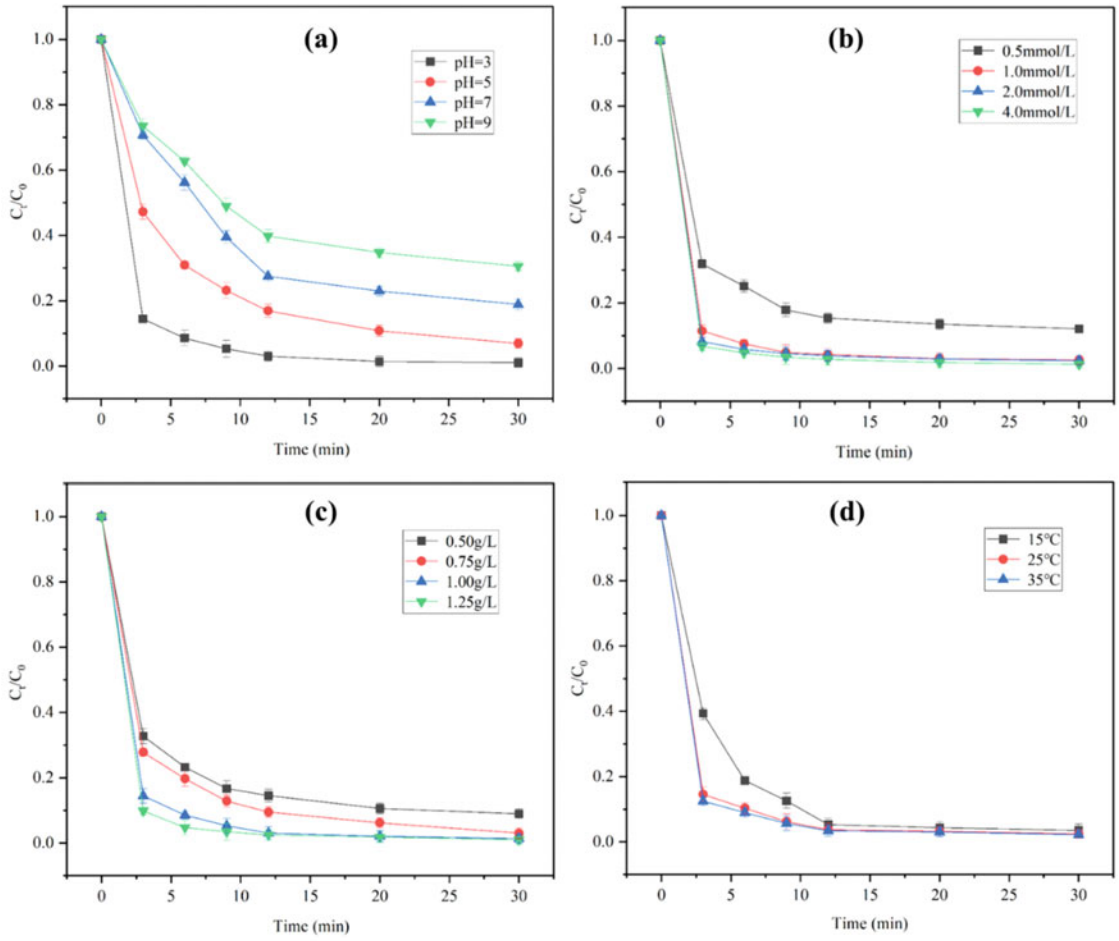

Figure 6. Effects of pH (a), H_2O_2 concentration (b), material dosage (c) and temperature (d) on tetracycline removal by ZVI-Cu/G

loss of active sites. The degradation effect of tetracycline decreased with the increase of pH of the solution, the removal rate of tetracycline decreased slightly, reaching 93% at pH = 5, 78% at pH = 7 and 66% at pH = 9. This may be because the passivation layer on the surface of ZVI is easier to form in alkaline environment, and excess OH^- ions react with O_2, Fe^{2+} and Fe^{3+} ions to form a passivation layer of iron hydroxide, which prevents the corrosion of ZVI and hinders the heterogeneous Fenton reaction. This finding is consistant with previous study in which the effect of pH value on the removal of β-naphthol orange by ZVI/Cu bimetal was discussed[23].

Effects of H_2O_2 concentration on tetracycline removal by ZVI-Cu/G

The experimental conditions in this section were set as follows: tetracycline concentration was 30 mg/L, the dosage of ZVI-Cu/G was 1.0 g/L, pH=3, and the temperature is 25 °C. The control variables of hydrogen peroxide concentrations were 0.5 mM, 1.0 mM, 2.0 mM and 4.0 mM, respectively. Figure 6b shows the tetracycline removal performance of ZVI-Cu/G at different hydrogen peroxide concentrations. When the concentration of hydrogen peroxide was 0.5 mM, the removal rate of tetracycline reached 90%. When the concentration of hydrogen peroxide increased to 1.0 mmol/L, the removal rate of tetracycline in the solution is significantly enhanced, reaching 98% in 30 min. When the hydrogen peroxide concentration reached 2.0 mM, 100% of tetracycline removal rate was achieved. When the hydrogen peroxide concentration was 4.0 mM, not much influence was shown on the improvement of tetracycline removal. It can be achieved when the hydrogen peroxide concentration reaches 2.0 mM. Previous study also reached a similar conclusion when using ZVI/Cu to remove sulfamethazine in water[24].

Effects of material dosage on tetracycline removal by ZVI-Cu/G

Experimental conditions in this section were set as follows: Tetracycline concentration was 30 mg/L, the concentration of hydrogen peroxide was 2.0 mM, pH = 3, and the temperature was 25 °C. The dosages of control variables were 0.50 g/L, 0.75 g/L, 1.00 g/L and 1.25 g/L, respectively. Figure 6c shows the effect of the ZVI-Cu/G dosage on tetracycline degradation. The tetracycline degradation has been completed after 30 min. When the dosage was 0.50 g/L, the tetracycline removal rate reached 85%. And as the dosage reached 0.75 g/L, the removal rate reached 97%. In the first 12 min, the reaction rate in the system with 1.25 g/L ZVI-Cu/G was faster than that with 1.00 g/L ZVI-Cu/G, but both of them finally removed 100% of the tetracycline. With the increase of ZVI amount, more Fe^{2+} will be released in the corrosion process, and these Fe^{2+} will catalyze the formation of •OH from H_2O_2, which will effectively oxidize tetracycline. To some extent, Fenton reagents will also increase and hydrogen peroxide will be more fully used. Previous study also found this phenomenon when using Cu/Fe amination polyacrylonitrile to remove 4-fluorophenol in water[25].

Effects of temperature on tetracycline removal by ZVI--Cu/G

Experimental conditions in this section were: TC concentration was 30 mg/L, the concentration of hydrogen peroxide was 2.0 mM, pH = 3, and the dosage of ZVI-Cu-/G was 1.00 g/L. The control variables temperature were 15 °C, 25 °C, and 35 °C, respectively. Figure 6d shows the TC degradation performances of ZVI-Cu/G material under different temperature conditions. The removal rate of tetracycline at different temperatures in the first 10 min was relatively rapid and reached equilibrium when the reaction time reached 12 min. The removal rate of tetracycline increased from 97% to 100% in 30 min, as the temperature increased from 15 °C to 25 °C. This may be due to the fact that higher temperature increases the rate of •OH formation according to Arrhenius law and improves the removal rate of tetracycline[26].

Reusability of ZVI-Cu/G

Figure 7 shows the reusing performance of ZVI-Cu/G, the tetracycline removal rate decreased with the increase of the number of repetitions. 90% of the tetracycline is degraded within the first 30 min of the fifth cycle, showing the promising reusability of this material. The concentrations of iron and copper ions in the solution were tested to further evaluate the metal-leaching ability of this material. The Fe and Cu concentrations in the solution after reusing are lower than 8.3 mg/L and 0.4 mg/L, respectively, very low metal leaching that supports the high stability observed (Table 2). Table 3 shows the tetracycline removal performances of various materials reported in the literature. It is noteworthy that ZVI-Cu/G catalyst shows very similar tetracycline degradation percentages or even higher than most of the materials previously reported. Based on estimation, the cost of improving ZVI to prepare ZVI-Cu/G is very low because the raw materials, i.e. spent LIBs are solid waste.

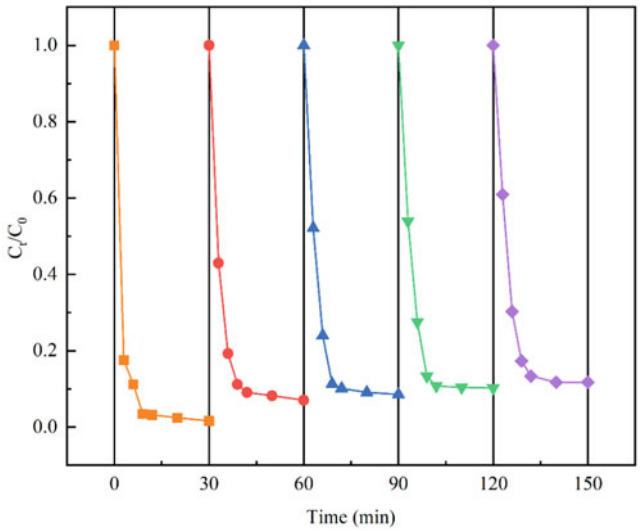

Figure 7. Reuse performances of ZVI-Cu/G

Table 2. Concentrations of metal ion in solutions of each reuse cycle

Cycle	1st	2nd	3rd	4th	5th
Fe ion (mg/L)	8.3	6.8	6.3	6.7	5.8
Cu ion (mg/L)	0.4	0.3	0.3	0.2	0.3

Table 3. TC removal performances of various materials

Catalyst	Removal percentage	Method	Condition	Ref.
ZVI-Cu/G	100%	Adsorption and heterogeneous Fenton	30 mg/L tetracycline, pH = 3, the 2.0 mM hydrogen peroxide, 1.00 g/L material, 25 ℃	This study
mZVI/N-doped graphene-like BC	100%	Fenton-like reactions	20 mg/L tetracycline, 60 min, 0.2 g/L material, 50 mL sluge, 35 °C, pH = 5-6.8	27
BC-supported sulfidated ZVI	100%	Adsorption and Fenton-like reactions	3 mg/L tetracycline, 120 min, 1.2 g/L material, 50 mM H_2O_2, pH = 7.2	28
3D printed ZVI@polylactic acid and persulfate	15%	Oxidation	100 mg/L tetracycline, 60 min, 3.3 g/L material, 1 mM SPS, 40 °C, pH = 3.5	14
sponge-Fe0@Cu-Pd trimetal and ambient oxygen	99%	Oxidation	30 mg/L tetracycline, 60 min, 25.52 g/L material, 25 °C, pH = 3	29
ZVI and air	94%	Adsorption, oxidation and reduction	20 mg/L tetracycline, 30 min, 0.4g/L ZVI, 500 mL/min air, pH = 2.5	30
Pistachio shell powder-ZVI and peroxymonosulfate	92%	oxidation	100 mg/L tetracycline, 24 h, 50 mg/L material, 100 mg/L of PMS, 25 °C, pH = 2	31

The main cost of preparing ZVI-Cu/G is from the power consumption of ball milling, showing that this catalyst is promising for the application of tetracycline removal.

Mechanism of tetracycline degradation by ZVI-Cu/G

The tetracycline degradation profiles were successfully fitted to a pseudo-first-order rate equation, as shown in Table 4. After the material enters the tetracycline solution, the main reaction equations are shown as Eq. 2–8:

$$Fe^0 + O_2 + 2H_2O \rightarrow Fe^{2+} + 4OH^- \quad (2)$$

$$Fe^0 + O_2 + 2H^+ \rightarrow Fe^{2+} + H_2O \quad (3)$$

$$Fe^0 + H_2O_2 + 2H^+ \rightarrow Fe^{2+} + 2OH^- \quad (4)$$

$$Fe^{2+} + H_2O_2 \rightarrow Fe^{3+} + \bullet OH + 4OH^{\bullet} \quad (5)$$

$$Fe^{3+} + H_2O_2 \rightarrow Fe^{2+} + O_2 + 2H^+ \quad (6)$$

$$Fe^{2+} + O_2 \rightarrow Fe^{3+} + \cdot O_2^- \quad (7)$$

$$H_2O_2 + \cdot OH \rightarrow HO_2 \cdot + H_2O \quad (8)$$

$$Fe^0 + 2Fe^{3+} \rightarrow 3Fe^{2+} \quad (9)$$

$$Cu^+ + Fe^{3+} \rightarrow Cu^{2+} + Fe^{2+} \quad (10)$$

$$Cu^+ + H_2O_2 \rightarrow Cu^{2+} + \bullet OH + OH^- \quad (11)$$

Firstly, Fe^0 can react with H_2O or/and H^+ to generate Fe^{2+}, and Fe^{2+} reacts with hydrogen peroxide to generate Fe^{3+}, and •OH attacks organic molecules unselectively. Further, The Fe^{3+} reacted with H_2O_2 to regenerate Fe^{2+}. These two reactions occurred continuously in Fenton-like reactions to form a cycle. ZVI-Cu on the surface of the material will form a galvanic cell, which will react on the surface to generate hydrogen. In the Fenton system, iron-copper bimetal can generate more hydroxyl radical (•OH), which improves the removal effect of tetracycline. Three different reaction by-products, with the m/z numbers of 117, 134 and 149, were detected. Tetracycline was firstly attacked by oxygen-containing free radicals and hydroxylates at the hydroxyl site to produce the intermediate with m/z of 461. Further, hydroxylation occurred at C12 to form the intermediate with m/z of 463. Then, demethylation occurred at the N4 site to form intermediate with m/z of 349. After that, the methylamino group fell off and the further degradation lead to the intermediate with m/z of 242. Finally, this intermediate underwent oxidation and break into smaller molecular intermediates with m/z of 134, 149, and 117, respectively, and further broken down into CO_2 and H_2O.

Table 4. Kinetic fitting results of pseudo-first order kinetic model for tetracycline removal in different conditions

Factors	Value	k (min^{-1})	R^2
pH	3	0.138	0.98
	5	0.076	0.98
	7	0.039	0.82
	9	0.035	0.78
H_2O_2 concentration	0.5 mM	0.037	0.95
	1.0 mM	0.091	0.94
	2.0 mM	0.123	0.99
	4.0 mM	0.249	0.96
Material dosage	0.50 g/L	0.063	0.98
	0.75 g/L	0.086	0.98
	1.00 g/L	0.132	0.99
	1.25 g/L	0.280	0.98
Temperature	15 ℃	0.075	0.96
	25 ℃	0.129	0.99
	35 ℃	0.1329	0.98

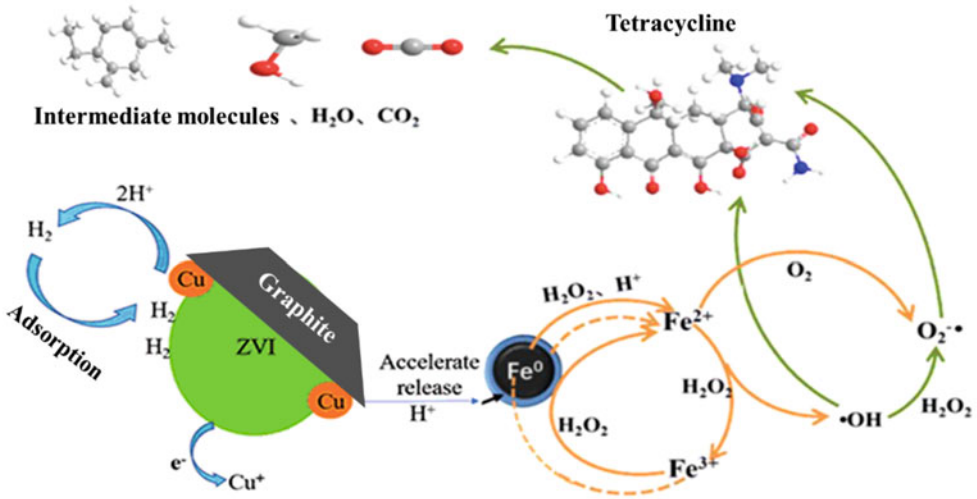

Figure 8. Mechanism of tetracycline degradation by ZVI-Cu/G

CONCLUSIONS

The ZVI-Cu/G was synthesized by using ZVI and graphite and copper from spent LIBs as raw materials and then prepared by ball milling method. The tetracycline degradation performances by ZVI-Cu/G increased with the decrease of pH value of the solution, with the increase of hydrogen peroxide concentration, with the increase of temperature, and with the increase of material dosage. Considering the reactivity and cost, when the tetracycline solution concentration was 30 mg/L, conditions included the initial pH was 3, the hydrogen peroxide concentration was 2.0 mM, the dosage was 1.00 g/L and the temperature was 25 °C were the best reaction conditions. The addition of Cu and graphite promoted the electron transfer between ZVI and tetracycline. The tetracycline removal process with ZVI-Cu/G material showed pseudo-first-order kinetic characteristics. Tetracycline removal was as high as 90% even in the third round of reuse, with low iron and copper lixiviation. The present study confirms the potential of using spent graphite and copper and ZVI to synthesize active and stable ZVI-Cu/G catalysts for the degradation of tetracycline in water. The benefit of using ZVI-Cu/G for tetracycline removal is the enhanced reactivity compared with ZVI. This higher reactivity can reduce the amount of ZVI used. The future study on ZVI-Cu/G may focus on the effects of copper dosage on its reactivity for tetracycline removal. Also, large-scale preparation of this catalyst should be evaluated.

ACKNOWLEDGEMENTS

We gratefully acknowledge China Ministry of Education Chunhui Programme (202200704), Shanghai Pujiang Programme (23PJD039), Open Fund of Anhui International Joint Research Center for Nano Carbon-based Materials and Environmental Health (NCMEH2022Y02), Shanghai Pudong New Area Science and Technology Development Fund Special Project for People's Livelihood Scientific Research (PKJ2023-C01).

LITERATURE CITED

1. Ordoñez, J., Gago, E.J. & Girard, A. (2016). Processes and technologies for the recycling and recovery of spent lithium-ion batteries. *Renew. Sustainable Energy Rev.* 60, 195–205. DOI: 10.1016/j.rser.2015.12.363.

2. Harper, G., Sommerville, R., Kendrick, E., Driscoll, L., Slater, P., Stolkin, R., Walton, A., Christensen, P., Heidrich, O., Lambert, S., Abbott, A., Ryder, K., Gaines, L. & Anderson, P. (2019). Recycling lithium-ion batteries from electric vehicles. *Nature,* 575(7781), 75–86. DOI: 10.1038/s41586-019-1682-5.

3. Chen, S., Li, Z., Belver, C., Gao, G., Guan, J., Guo, Y., Li, H., Ma, J., Bedia, J. & Wójtowicz, P. (2020). Comparison of the behavior of ZVI/carbon composites from both commercial origin and from spent Li-ion batteries and mill scale for the removal of ibuprofen in water. *J. Environ. Manag.* 264, 110480. DOI: 10.1016/j.jenvman.2020.110480.

4. Zhao, T., Yao, Y., Wang, M., Chen, R., Yu, Y., Wu, F. & Zhang, C. (2017). Preparation of MnO_2-modified graphite sorbents from spent Li-ion batteries for the treatment of water contaminated by lead, cadmium, and silver. *ACS Appl. Mater. & Interf.* 9(30), 25369–25376. DOI: 10.1021/acsami.7b07882.

5. Anh Nguyen, T.-H. & Oh, S.-Y. (2021). Anode carbonaceous material recovered from spent lithium-ion batteries in electric vehicles for environmental application. *Waste Management*, 120, 755–761. DOI: 10.1016/j.wasman.2020.10.044.

6. Yan, L., Song, X., Miao, J., Ma, Y., Zhao, T. & Yin, M. (2024). Removal of tetracycline from water by adsorption with biochar: A review. *J. Water Process Engin.* 60, 105215. DOI: 10.1016/j.jwpe.2024.105215.

7. Mostafapour, F.K., Yilmaz, M., Mahvi, A.H., Younesi, A., Ganji, F. & Balarak, D. (2022). Adsorptive removal of tetracycline from aqueous solution by surfactant-modified zeolite: Equilibrium, kinetics and thermodynamics. Desalination and Water Treatment, 247, 216–228. DOI: 10.5004/dwt.2022.27943.

8. Ortiz-Ramos, U., Leyva-Ramos, R., Mendoza-Mendoza, E., Carrasco-Marín, F., Bailón-García, E., Villela-Martínez, D.E. & Valdez-García, G.D. (2024). Modeling adsorption rate of trimethoprim, tetracycline and chlorphenamine from aqueous solutions onto natural bentonite clay: Elucidating mass transfer mechanisms. *Chem. Engin. J.* 493, 152666. DOI: 10.1016/j.cej.2024.152666.

9. Ali, M.M.M., Ahmed, M.J. & Hameed, B.H. (2018). Nay zeolite from wheat (*triticum aestivum l.*) straw ash used for the adsorption of tetracycline. *J. Cleaner Prod.* 172, 602–608. DOI: 10.1016/j.jclepro.2017.10.180.

10. Sun, B., Sun, M., Zhang, J., Zhao, F., Shao, C., Yi, M., Wang, Y., Wang, X., Zhu, S. & Cai, X. (2023). Effective adsorption of tetracycline by Fe-Mn-Ce composite metal oxides: Kinetics, isotherm and mechanism. Desalination and Water Treatment, 308, 190–199. DOI: 10.5004/dwt.2023.29819.

11. Selvaraj, R., Jogi, S., Murugesan, G., Srinivasan, N.R., Goveas, L.C., Varadavenkatesan, T., Samanth, A., Vinayagam, R., Ali Alshehri, M. & Pugazhendhi, A. (2024). Machine

learning and statistical physics modeling of tetracycline adsorption using activated carbon derived from cynometra ramiflora fruit biomass. *Environ. Res*. 252, 118816. DOI: 10.1016/j.envres.2024.118816.

12. Hamdi, S., Gharbi-Khelifi, H., Barreiro, A., Mosbahi, M., Cela-Dablanca, R., Brahmi, J., Fernández-Sanjurjo, M.J., Núñez-Delgado, A., Issaoui, M. & Álvarez-Rodríguez, E. (2024). Tetracycline adsorption/desorption by raw and activated tunisian clays. *Environ. Res.* 242, 117536. DOI: 10.1016/j.envres.2023.117536.

13. Li, X., Fu, W., Guan, R., Yuan, Y., Zhong, Q., Yao, G., Yang, S.-T., Jing, L. & Bai, S. (2024). Nucleophiles promotes the decomposition of electrophilic functional groups of tetracycline in ZVI/H_2O_2 system: Efficiency and mechanism. *Chin. Chem. Letters*, 35(10), 109625. DOI: 10.1016/j.cclet.2024.109625.

14. Fernández-Velayos, S., Sánchez-Marcos, J., Munoz-Bonilla, A., Herrasti, P., Menéndez, N. & Mazarío, E. (2022). Direct 3D printing of zero valent iron@polylactic acid catalyst for tetracycline degradation with magnetically inducing active persulfate. *Sci. Total Environ.* 806, 150917. DOI: 10.1016/j.scitotenv.2021.150917.

15. Zhang, X., Ding, Y., Tang, H., Han, X., Zhu, L. & Wang, N. (2014). Degradation of bisphenol a by hydrogen peroxide activated with $CuFeO_2$ microparticles as a heterogeneous fenton-like catalyst: Efficiency, stability and mechanism. *Chem. Engin. J.* 236, 251–262. DOI: 10.1016/j.cej.2013.09.051.

16. Liu, Y.-L., Zhang, C., Guo, L., Zeng, Q., Wang, R., Chen, H., Zhang, Q. & Zeng, Q. (2023). Synergistically adsorbing and reducing uranium from water by a novel nano zero-valent copper/mxene 0D/2D nanocomposite. *Water Res*. 245, 120666. DOI: 10.1016/j.watres.2023.120666.

17. Zhou, L.Y., Chen, S., Li, H., Guo, S., Liu, Y.D. & Yang, J. (2018). EDDS enhanced *shewanella putrefaciens* CN32 and α-FeOOH reductive dechlorination of carbon tetrachloride. *Chemosphere,* 198, 556–564. DOI: 10.1016/j.chemosphere.2018.01.083.

18. Yang, Z., Liu, J., Yang, S., Fan, D. & Fu, P. (2023). Graphite-modified zero-valent aluminum prepared by mechanical ball milling for selective removal of hydrophobic carbon tetrachloride. *Chem. Engin. J*. 474, 145591. DOI: 10.1016/j.cej.2023.145591.

19. Islam, M., Arya, N., Weidler, P.G., Korvink, J.G. & Badilita, V. (2020). Electrodeposition of chitosan enables synthesis of copper/carbon composites for H_2O_2 sensing. *Mat. Today Chem.* 17, 100338. DOI: 10.1016/j.mtchem.2020.100338.

20. Yoshino, H., Kurosu, S., Yamaguchi, R. & Kawase, Y. (2018). A phenomenological reaction kinetic model for Cu removal from aqueous solutions by zero-valent iron (ZVI). *Chemosphere*, 200, 542–553. DOI: 10.1016/j.chemosphere.2018.02.127.

21. Garrido-Ramírez, E.G., Theng, B.K.G. & Mora, M.L. (2010). Clays and oxide minerals as catalysts and nanocatalysts in fenton-like reactions — A review. *Appl. Clay Sci.* 47(3), 182–192. DOI: 10.1016/j.clay.2009.11.044.

22. Lin, S.H., Lin, C.M. & Leu, H.G. (1999). Operating characteristics and kinetic studies of surfactant wastewater treatment by fenton oxidation. *Water Res*. 33(7), 1735–1741. DOI: 10.1016/S0043-1354(98)00403-5.

23. Yamaguchi, R., Kurosu, S., Suzuki, M. & Kawase, Y. (2018). Hydroxyl radical generation by zero-valent iron/Cu (ZVI/Cu) bimetallic catalyst in wastewater treatment: Heterogeneous Fenton/Fenton-like reactions by fenton reagents formed in-situ under oxic conditions. *Chem. Engin. J.* 334, 1537–1549. DOI: 10.1016/j.cej.2017.10.154.

24. Adel, A., Gar Alalm, M., El-Etriby, H.K. & Boffito, D.C. (2020). Optimization and mechanism insights into the sulfamethazine degradation by bimetallic ZVI/Cu nanoparticles coupled with H_2O_2. *J. Environ. Chem. Engin.* 8(5), 104341. DOI: 10.1016/j.jece.2020.104341.

25. Wang, X., Wang, P., Wang, Q., Xu, P., Yang, C., Xin, Y. & Zhang, G. (2021). Efficient degradation of 4-fluorophenol under dielectric barrier discharge plasma treatment using Cu/Fe-AO-PAN catalyst: Role of H_2O_2 production. *Chem. Engin. J*. 420, 127577. DOI: 10.1016/j.cej.2020.127577.

26. Gao, G., Li, Z., Chen, S., Belver, C., Lin, D., Li, Z., Guan, J., Guo, Y. & Bedia, J. (2023). Synthesis of zero-valent iron supported with graphite and plastic based carbon from recycling spent lithium ion batteries and its reaction mechanism with 4-chlorophenol in water. *J. Environ. Manag.* 325, 116490. DOI: 10.1016/j.jenvman.2022.116490.

27. Zhang, X., Sun, W., Wang, Y., Li, Z., Huang, X., Li, T. & Wang, H. (2024). Mechanochemical synthesis of microscale zero-valent iron/N-doped graphene-like biochar composite for degradation of tetracycline via molecular O_2 activation. *J. Colloid Interf. Sci.* 659, 1015–1028. DOI: 10.1016/j.jcis.2024.01.061.

28. Wang, A., Hou, J., Feng, Y., Wu, J. & Miao, L. (2022). Removal of tetracycline by biochar-supported biogenetic sulfidated zero valent iron: Kinetics, pathways and mechanism. *Water Res.* 225, 119168. DOI: 10.1016/j.watres.2022.119168.

29. Zhou, C., Lv, G., Zou, X., Wang, J., Chen, Y., Shen, J., Su, S., Xing, W., Fan, D. & Shen, Y. (2024). Construction of core–shell coordination sponge-Fe^0@Cu-Pd trimetal for high efficient activation of room-temperature dissolved ambient oxygen toward synergistic catalytic degradation of tetracycline and p-nitrophenol. *Separ. Purific. Technol.* 329, 125195. DOI: 10.1016/j.seppur.2023.125195.

30. Cao, J., Xiong, Z. & Lai, B. (2018). Effect of initial pH on the tetracycline (TC) removal by zero-valent iron: Adsorption, oxidation and reduction. *Chem. Engin. J.* 343, 492–499. DOI: 10.1016/j.cej.2018.03.036.

31. Kaur, P., Kumar, A., Babu, J.N. & Kumar, S. (2023). Tetracycline removal via three-way synergy between pistachio shell powder, zerovalent copper or iron, and peroxymonosulfate activation. *J. Hazard. Mat. Adv.* 12, 100385. DOI: 10.1016/j.hazadv.2023.100385.